Mineralogical Magazine, April 2010, Vol. 74(2), pp. 365–373

Eringaite, $Ca_3Sc_2(SiO_4)_3$, a new mineral of the garnet group

I. O. GALUSKINA[1,*], E. V. GALUSKIN[1], B. LAZIC[2], T. ARMBRUSTER[2], P. DZIERŻANOWSKI[3], K. PRUSIK[4] AND R. WRZALIK[5]

[1] Department of Geochemistry, Mineralogy and Petrography, Faculty of Earth Sciences, University of Silesia, Będzińska 60, 41-200 Sosnowiec, Poland
[2] Mineralogical Crystallography, Institute of Geological Sciences, University of Bern, Freiestr. 3, CH-3012 Bern, Switzerland
[3] Institute of Geochemistry, Mineralogy and Petrology, University of Warsaw, al. Żwirki i Wigury 93, 02-089 Warszawa, Poland
[4] Institute of Materials Science, University of Silesia, Bankowa 12, 40-007 Katowice, Poland
[5] Institute of Physics, University of Silesia, Uniwersytecka 4, 40-007 Katowice, Poland

[*Received 19 February 2010; Accepted 12 May 2010*]

ABSTRACT

Eringaite, $Ca_3Sc_2(SiO_4)_3$, a new mineral of the garnet group, is an accessory mineral in metasomatic rodingite-like rocks from the Wiluy River, Sakha-Yakutia Republic, Russia. Eringaite forms regular growth zones and irregular spots in complex garnet crystals containing a kimzeyite core. An electron back-scatter diffraction pattern with an excellent match to a garnet model with a = 12.19 Å was obtained for a grain with the largest Sc_2O_3 content having the crystal chemical formula $(Ca_{2.98}Y_{0.01}Mg_{0.01})_{\Sigma3}(Sc_{0.82}Ti^{4+}_{0.44}Fe^{3+}_{0.30}Zr_{0.21}Mg_{0.10}Al_{0.09}Cr^{3+}_{0.08}Fe^{2+}_{0.05}V^{3+}_{0.01})_{\Sigma2.01}(Si_{2.48}Al_{0.30}Fe^{3+}_{0.22})_{\Sigma3}O_{12}$. Eringaite is light brown to yellow with a creamy white streak. The crystals are transparent with a vitreous lustre. The calculated density of eringaite is 3.654 g cm^{-3}. The following main modes of the Raman spectrum are characteristic of eringaite: 335, 511, 735, 880 and 937 cm^{-1}. The strongest lines of the calculated powder diffraction data are as follows [(*hkl*) d_{hkl} (*I*)] (400) 3.064 (69), (420) 2.740 (100), (422) 2.502 (68), (640) 1.670 (30), (642) 1.638 (82), (840) 1.370 (20), (842) 1.137 (19), (10.4.2) 1.119 (29).

KEYWORDS: eringaite, scandium, garnet group, EBSD, single-crystal, Raman, Wiluy River, Sakha-Yakutia Republic, Russia.

Introduction

THE finding of Ti-Zr garnets with Sc_2O_3 of ~6 wt.% in unusual achtarandite-bearing aposkarn rodingite-like rocks from the Wiluy River, Sakha-Yakutia Republic, Russia (Galuskina *et al*., 2005) was the starting point for subsequent systematic investigations of garnet-group minerals from this occurrence. These led to the discovery of a new garnet – eringaite (scandian analogue of andradite) – with the empirical formula $(Ca_{2.98}Y_{0.01}Mg_{0.01})_{\Sigma3}(Sc_{0.82}Ti^{4+}_{0.44}Fe^{3+}_{0.30}Zr_{0.21}Mg_{0.10}Al_{0.09}Cr^{3+}_{0.08}Fe^{2+}_{0.05}V^{3+}_{0.01})_{\Sigma2}(Si_{2.48}Al_{0.30}Fe^{3+}_{0.22})_{\Sigma3}O_{12}$ and with end-member formula $Ca_3Sc_2(SiO_4)_3$.

Eringaite is one of rather few natural silicates containing significant scandium in their composition (Semenov *et al*., 1965; Mellini *et al*., 1982; Orlandi *et al*., 1998; Demartin *et al*., 2000; Raade *et al*., 2002; Gramaccioli *et al*., 2004; Pezzotta *et al*., 2005; Cooper *et al*., 2006; Ma and Rossman, 2009). The synthetic end-member analogue, $Ca_3Sc_2Si_3O_{12}$, of eringaite is well known (Mill', 1964, 1966; Mill' *et al*., 1977; Ito and Frondel, 1968; Woodland and Angel, 1996). Studies of synthetic garnets of the $Ca_3Fe_2Si_3O_{12}$–$Ca_3Sc_2Si_3O_{12}$ series indicate that Sc occupies

* E-mail: irina.galuskina@us.edu.pl
DOI: 10.1180/minmag.2010.074.2.365

the octahedral site. Synthetic $Ca_3Sc_2Si_3O_{12}$ doped with *REE* and other elements has technological applications as luminescence materials, lasers etc. (Chen *et al*., 2009; Ivanovskikh *et al*., 2010).

Eringaite was approved by the International Mineralogical Association's Commission on New Minerals, Nomenclature and Classification in October 2009. The name eringaite originates from the Eringa River, the tributary of the Wiluy River (Offman and Novikova, 1955). The rodingite rocks containing eringaite occur on the north-western bank of the Wiluy River opposite its junction with the Eringa river. The type specimen No. 3837/1 is deposited in the collection of the Fersman Mineralogical Museum in Moscow (Russia).

Methods of investigation

Investigations of the composition and morphology of the eringaite and associated minerals, and the selection of grains for Raman and structural studies, were performed using a scanning electron microscope Philips XL30 (University of Silesia, Poland) operated either at high vacuum (HV) or low vacuum (LV). Garnet compositions were determined using a microprobe analyser CAMECA SX100 (University of Warsaw, Poland) at 15 kV, 40–50 nA, and a beam diameter of 1–3 μm. Natural and synthetic standards were used: wollastonite – Ca-*K*α; diopside – Mg-*K*α, Ca-*K*α, Si-*K*α; andradite – Si-*K*α; Sc_2O_3 – Sc-*K*α; hematite – Fe-*K*α; orthoclase – Al-*K*α; rutile – Ti-*K*α; zircon – Zr-*L*α; HfO_2 – Hf-*M*α; $Y_3Al_5O_{12}$ – Y-*L*α; V_2O_5 – V-*K*α; Cr_2O_3 – Cr-*K*α; rhodonite – Mn-*K*α. Corrections were applied using the CAMECA 'PAP' procedure (Pouchou and Pichoir, 1985).

Based on electron microprobe analyses, a small (0.02 mm × 0.02 mm × 0.03 mm) crystal, of $(Ca_{3.00}Y_{0.01})_{\Sigma 3.009}(Sc_{0.63}Ti^{4+}_{0.66}Fe^{3+}_{0.25}Zr_{0.30}Mg_{0.08}Cr^{3+}_{0.06}Fe^{2+}_{0.01})\Sigma_{1.99}(Si_{2.13}Al_{0.26}Fe^{3+}_{0.61})_{\Sigma 3}O_{12}$ composition, was studied using an APEX II SMART single-crystal diffractometer (University of Bern, Switzerland), Mo-*K*α (λ = 0.71073 Å) X-radiation at 50 kV, 35 mA.

The size of the eringaite crystal with the greatest Sc_2O_3 content did not exceed 10 μm. Thus, the symmetry and cell parameters of this garnet were determined by electron back-scatter diffraction (EBSD) using a high-performance scanning electron microscope JSM-6480 equipped with EBSD (University of Silesia, Poland). The EBSD images were recorded with a HKL Nordlys II camera using a 30 kV beam energy. Composition measurements were performed on microprobe thin sections re-polished with an Al_2O_3 suspension of 20 nm particle size. Calibration of the geometry of the SEM and EBSD system was carried out on Si for two detector distances, i.e. 177 mm (normal working position) and 150 mm (camera refracted position). The program *Channel5* (Day and Trimby, 2004) was used for the interpretation of the EBSD diffraction patterns.

Raman spectra of single eringaite crystals were recorded using a LabRam System spectrometer (Jobin-Yvon-Horiba, University of Silesia, Poland). The incident laser excitation was provided by a water-cooled argon laser source operating at 514.5 nm. The power at the exit of a 100× objective lens varied from 20 to 40 mW. In order to avoid undesirable Rayleigh scattering, two notch-filters were used, cutting the laser line at 200 cm^{-1}. The Raman spectra were recorded in 0º geometry, in the range of 200–4000 cm^{-1} Raman shift and with a spectral resolution of 3.5 cm^{-1}. A collection time of 60 s was chosen and 4–10 scans were accumulated. The monochromator was calibrated using the Raman scattering line of a silicon plate (520.7 cm^{-1}).

Occurrence and description of eringaite

Calcium garnets of the schorlomite–kimzeyite series with large Sc_2O_3 contents occur in a large xenolith of grossular-vesuvianite rodingite-like aposkarn rocks intercalated with serpentinites and chlorite rocks hosted in the ~250 Ma Erbeekskaya gabbro-dolerite intrusion (Lyakhovich, 1954, Oleynikov, 1979) cropping out at the Wiluy River, Sakha-Yakutia Republic, Russia (Galuskina *et al*., 2005). This intrusion belongs to the Siberian trap formation. These unusual metasomatic rocks on the shores of the Wiluy River 7 km to the west of the Chernyshevsky settlement (63.0 N, 112.3 E) are also the type locality of grossular (Werner, 1811) and wiluite (Prendel, 1887; Groat *et al*., 1998). In addition, achtarandite of tetrahedral habit, a pseudomorph of hibschite after wadalite, is commonly a main rock-forming mineral in the rock (Galuskina *et al*., 1998).

In these rodingite-like rocks, grossular and vesuvianite associated with abundant serpentine form peculiar symplectitic pseudomorphs after a tabular mineral which probably belongs to the melilite group (Fig. 1*a*). Thus, a high-temperature

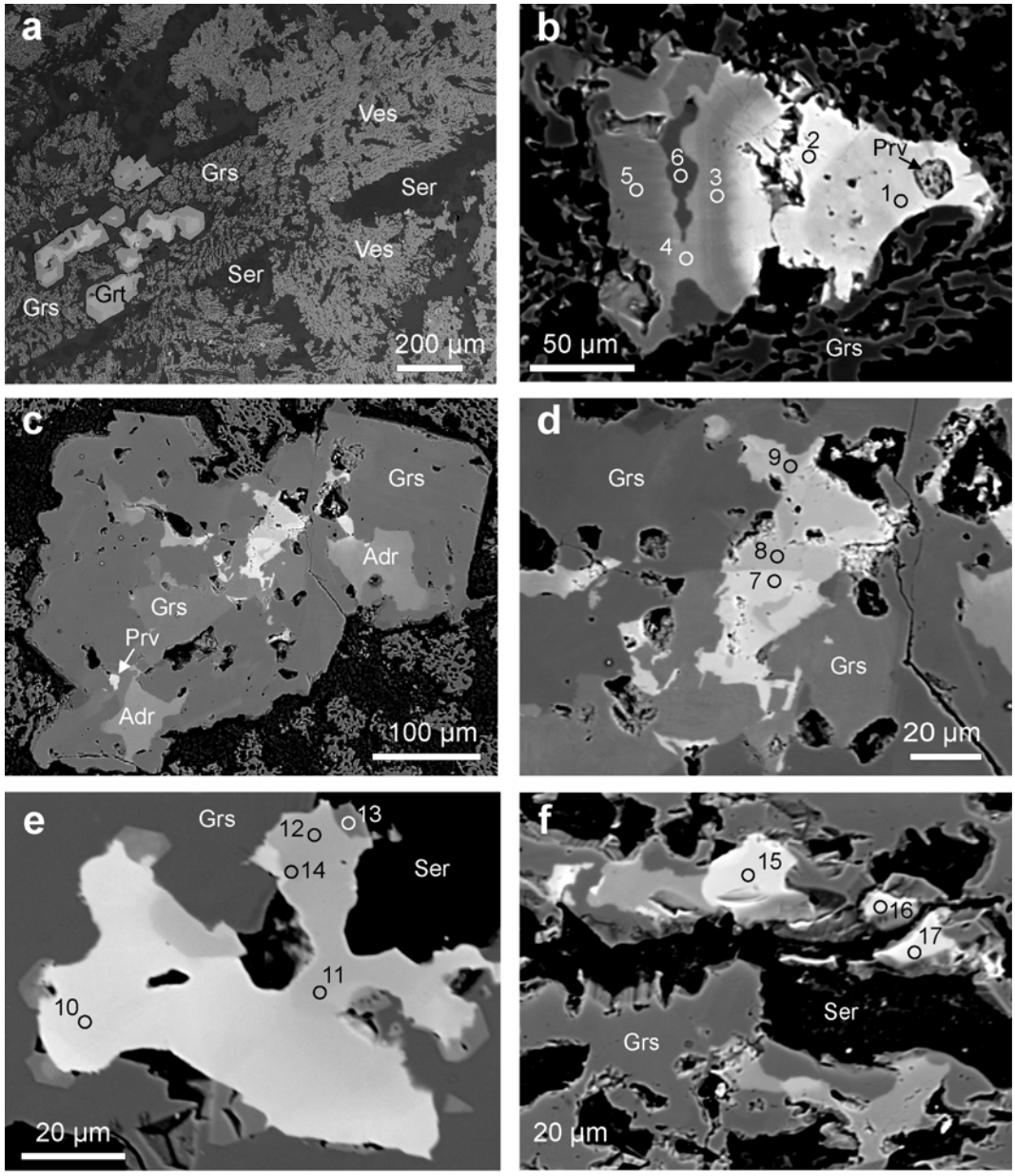

FIG. 1. (*a*) Rodingite-like rock with grossular (Grs)-vesuvianite (Ves) symplectites after melilite group minerals and garnet crystals with complex zones (Grt) containing Sc-bearing zones. The space between garnet and vesuvianite is filled by serpentine (Ser) with minor chlorite and calcite. (*b*) Zoned garnet crystal with regular growth zone of eringaite and perovskite (Prv) inclusion. (*c*) Large grossular crystal with andradite (Adr) domains and an irregular spot of eringaite. (*d*) Magnified area of central part of crystal shown in *c*. (*e*) Irregular complex garnet crystal containing a discrete spot of eringaite with maximum Sc_2O_3 content. (*f*) Irregular eringaite grain used for single-crystal X-ray investigation.

melilite skarn was probably the primary rock (Galuskina *et al*., 2005). Unaltered åkermanite and boron-bearing gehlenite also occur as inclusions in grossular and wiluite in other zones of these achtarandite skarns (Galuskin, 2005). Accessory minerals are diopside and fassaitic pyroxene, wiluite, perovskite, zircon, baghdadite, magnetite, hematite, titanite, fluorapatite, chlorite of the clinochlore–chamosite series and calcite. The achtarandite pseudomorphs suggest that wadalite was one of the early minerals (Galuskina *et al*., 1998).

Eringaite is light brown to yellow with a creamy white streak. The crystals are transparent and have vitreous lustre. The mineral has no cleavage and its fracture is irregular. Hardness was not determined due to the small crystal size. The calculated density is 3.654 g cm^{-3}.

Results

Eringaite forms either regular growth zones or irregular spots (<10 μm) in garnet crystals of complex composition (Fig. 1). From core to rim, the following zones can be distinguished (Fig. 1*b*): (1) kimzeyite and/or zirconian schorlomite (Table 1, analyses 1, 2); (2) titanian-zirconian eringaite and/or scandian-zirconian schorlomite (Table 1, analysis 3); (3) zirconian schorlomite and/or kimzeyite (Table 1, analysis 4); (4) titanian Zr-bearing andradite (Table 1, analysis 5); and (5) grossular (Table 1, analysis 6). Commonly, a primary zonation is disturbed by later processes. Garnet crystals are often covered by a thin hibschite zone (Galuskin, 2005). Irregular relics of eringaite and kimzeyite–schorlomite occur in the central parts of large grossular crystals along with spots of ferrian grossular and andradite enriched in Ti and Zr resulting from the metasomatic substitution of early garnet (Fig. 1*c*,*d*; Table 1).

The Sc_2O_3 present in varying quantities in all garnet zones of the kimzeyite–schorlomite–andradite series (Table 1, Fig. 1*b–f*) is inherited from the primary high-temperature melilite skarns. Later garnet zones belonging to the andradite–grossular series, and also the last-formed hibschite, still contain trace amounts of scandium (Table 1).

As a rule of thumb, a garnet crystal from this locality with regular zonation and a kimzeyite or zirconian schorlomite core will probably feature a zone of significant scandium content (Sc_2O_3 > 8 wt.%). Large Sc contents are not seen in the

TABLE 1. Chemical composition (wt.%) of eringaite and associated garnets.

	– Eringaite holotype –			1	2	3	4	5	6	7	8	9	10	11	12	13	14	15*	16	17
	Mean 8	s.d.	Range			Fig. 1*b*					Fig. 1*d*				Fig. 1*e*				Fig. 1*f*	
SiO_2	29.39	0.16	29.12–29.61	19.76	16.65	27.26	23.41	29.70	34.71	20.86	25.02	25.15	21.07	26.32	27.97	38.28	29.61	24.18	27.15	27.29
TiO_2	7.17	0.42	6.85–8.14	9.96	9.80	9.58	9.88	8.47	4.86	9.93	9.64	9.63	10.82	10.33	9.37	1.76	7.01	9.96	9.69	9.26
ZrO_2	5.28	0.13	5.03–5.41	13.63	18.48	5.79	8.01	1.47	1.35	12.37	7.68	7.49	12.89	7.19	6.04	1.12	5.20	6.96	5.01	5.75
HfO_2	0.14	0.01	0.12–0.16	0.46	0.38	0.13	0.24	0.10	0.09	0.23	0.16	0.19	0.34	0.16	0.15	0.05	0.14	0.16	0.10	0.14
Al_2O_3	3.15	0.07	3.06–3.25	3.39	3.98	3.51	0.15	5.16	10.72	3.19	3.00	3.05	4.47	3.66	3.96	13.40	3.06	2.53	3.56	3.49
Sc_2O_3	10.67	0.40	9.92–11.20	1.00	0.52	7.94	3.02	0.19	0.19	3.43	8.01	7.59	2.79	6.16	7.01	0.52	11.20	8.17	8.50	7.42
Y_2O_3	0.20	0.04	0.15–0.29	n.d.	n.d.	n.d.	0.07	n.d.	n.d.	0.13	0.14	0.20	0.14	0.16	0.15	n.d.	0.29	0.16	0.18	0.11
V_2O_3	0.14	0.05	0.06–0.23	n.d.	n.d.	n.d.	1.44	0.10	n.d.	0.04	0.07	0.08	n.d.	0.11	0.12	n.d.	0.12	n.d.	0.08	0.01
Cr_2O_3	1.05	0.05	0.99–1.13	2.65	1.22	0.56	1.83	1.71	0.42	1.72	0.62	0.60	0.82	0.56	0.64	0.11	1.13	0.83	0.93	0.53
Fe_2O_3	8.48	0.51	8.01–9.49	16.41	17.08	10.54	18.54	18.05	10.99	15.6	12.26	12.82	14.20	11.37	10.32	8.84	8.17	13.00	9.76	10.78
FeO	0.50	0.26	0.04–0.88	0.51	0.63	0.27				0.53			0.41	0.41	0.88	0.09	0.67	0.14	0.42	
MnO	0.01	0.01	0–0.03	n.d.	n.d.	0.06		n.d.	0.06	n.d.	n.d.	n.d.		0.04	n.d.	0.04	n.d.	n.d.	0.05	0.03
CaO	33.19	0.25	32.62–33.45	30.68	29.81	32.67	31.31	33.17	34.93	30.98	32.4	32.46	31.48	32.90	32.82	35.90	33.27	31.78	32.44	32.68
MgO	0.95	0.07	0.84–1.08	0.56	0.45	1.37	0.69	0.89	1.52	0.56	0.86	0.86	1.02	1.35	1.41	1.07	0.84	0.63	1.21	1.47
Total	100.31	0.53	99.44–100.96	99.23	99.00	99.68	98.59	99.15	99.84	99.57	99.86	100.12	100.45	100.72	100.84	101.18	100.71	98.50	99.07	98.96

Calculated on 12O and Fe^{3+}/Fe^{2+} ratio calculated on charge balance																		
Ca	2.99	3.00	3.00	2.98	2.99	2.99	3.00	2.99	3	3	2.99	3	2.95	2.98	2.98	3.00	2.97	3
Y	0.01				0.01			0.01	0.01	0.01	0.01	0.01	0.01		0.01	0.01	0.01	
Mg				0.02		0.01							0.04	0.02	0.01		0.02	
X-site	3	3	3	3	3	3	3	3	3.01	3.01	3	3.01	3	3	3	3.01	3	3
Ti^{4+}	0.45	0.68	0.69	0.61	0.66	0.54	0.29	0.67	0.63	0.63	0.72	0.66	0.59	0.10	0.44	0.66	0.62	0.60
Zr	0.22	0.62	0.85	0.24	0.35	0.06	0.05	0.54	0.32	0.32	0.56	0.30	0.25	0.04	0.21	0.30	0.21	0.24
Hf		0.01	0.01		0.01			0.01			0.01							
Sc	0.78	0.08	0.04	0.59	0.11	0.02	0.02	0.27	0.60	0.57	0.21	0.45	0.51	0.04	0.82	0.63	0.63	0.55
Fe^{3+}	0.32	0.30	0.21	0.35	0.64	1.15	0.66	0.27	0.28	0.31	0.28	0.33	0.40	0.51	0.30	0.25	0.31	0.38
Al						0.01	0.79							1.19				
Cr^{3+}	0.07	0.19	0.09	0.04	0.13	0.11	0.03	0.12	0.04	0.04	0.06	0.04	0.04	0.01	0.08	0.06	0.06	0.04
V^{3+}	0.01				0.01	0.01			0.01	0.01		0.01	0.01		0.01		0.01	
Mg	0.12	0.08	0.06	0.15	0.09	0.10	0.18	0.08	0.11	0.11	0.13	0.17	0.14	0.10	0.10	0.08	0.13	0.19
Fe^{2+}	0.03	0.04	0.05	0.02				0.04			0.03	0.03	0.06	0.01	0.05	0.01	0.03	
Y-site	2	2	2	2	2	2	2.02	2	1.99	1.99	2	1.99	2	2	2.01	1.99	2	2
Si	2.47	1.81	1.56	2.32	2.09	2.50	2.78	1.88	2.17	2.17	1.86	2.24	2.35	2.97	2.48	2.13	2.32	2.34
Al	0.31	0.36	0.44	0.35	0.31	0.50	0.22	0.34	0.31	0.31	0.47	0.37	0.39	0.03	0.30	0.26	0.36	0.35
Fe^{3+}	0.22	0.83	1.00	0.33	0.60			0.78	0.52	0.52	0.67	0.39	0.26		0.22	0.61	0.32	0.31
Z-site	3	3	3	3	3	3	3	3	3	3	3	3	3	3	3	3	3	3
Erg	39**	4	2	29.5	5.5	1	1	13.5	30.2	28.6	10.5	22.6	25.5	2	40.8	31.7	31.5	27.5
Adr	16	15	10.5	12	32	35.5	24.3	13.5	14.1	15.6	14	13.1	13	25.5	14.9	12.6	8	13.5
Uvr	4	9.5	4.5	2	7	6	1.5	6	2.5	2.5	3	2.5	2.5	0.5	4.5	3	3.5	2
Grs				5.5		22.5	47.5					3.5	7	59.5			7.5	5.5
Σ	59	28.5	17	49	44.5	65	74.3	33	46.8	46.7	27.5	41.7	48	87.5	60.2	47.3	50.5	48.5
Mrt	15	12	11	17	9	10	17.8	12	11.1	11.1	16	20.1	20	11	14.9	9	16	19
Schr	15	28	29	22	28.5	22	5.4	27.5	26.1	26.1	28	23.1	19.5		14.4	28.6	23	20.5
Kmz	11	31.5	43	12	18	3	2.5	27.5	16	16.1	28.5	15.1	12.5	1.5	10.5	15.1	10.5	12
Σ	26	59.5	72	34	45	25	7.9	55	42.1	42.2	56.5	38.2	32	1.5	24.9	43.7	33.5	32.5

* – crystal used for single-crystal X-ray investigation (mean 4); ** – underlined end-member determines garnet name; Erg – eringaite $Ca_3Sc_2Si_3O_{12}$, Adr – andradite $Ca_3Fe_2^{3+}Si_3O_{12}$, Uvr – sum of uvarovite $Ca_3Cr_2^{3+}Si_3O_{12}$ and goldmanite $Ca_3V_2^{3+}Si_3O_{12}$, Grs – grossular $Ca_3Al_2Si_3O_{12}$, Mrt – sum of morimotoite $Ca_3Fe^{2+}Ti^{4+}Si_3O_{12}$ and morimotoite-Mg $Ca_3MgTi^{4+}Si_3O_{12}$ (Locock, 2008), Schr – sum of schorlomite $Ca_3Ti_2^{4+}Fe_2^{3+}SiO_{12}$ and schorlomite-Al $Ca_3Ti_2^{4+}Al_2SiO_{12}$, Kmz – sum of kimzeyite $Ca_3Zr_2Al_2SiO_{12}$ and kimzeyite-Fe (IMA2009-029) $Ca_3Zr_2Fe_2^{3+}SiO_{12}$.

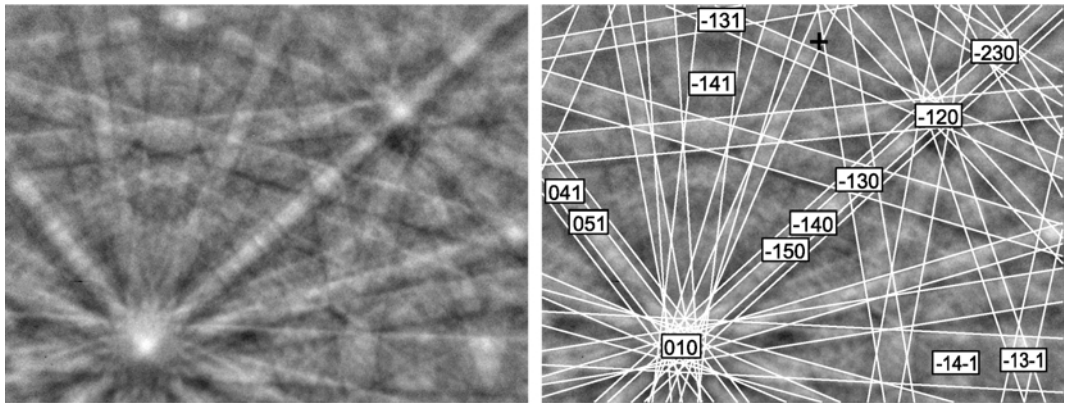

FIG. 2. EBSD pattern of eringaite and fitting result at a detector distance of 150 mm.

core of the garnet. The Zr content in the Sc-rich zone increases towards the rim (Fig. 1*b*, Table 1). The maximum Sc_2O_3 content (11.20 wt.%) was established in eringaite spots up to 10 μm in size within complex crystals (Fig. 1*e*, Table 1).

Because of limited data, due to the small crystal size, structure refinements were done with isotropic displacement parameters. The structure refinement data obtained were not satisfactory and are omitted from this paper. Single-crystal X-ray diffraction confirmed space group $Ia\bar{3}d$ with a = 12.255(1) Å, V = 1840.52(6) Å^3 and Z = 8 for a grain of scandian garnet (Fig. 1*f*) of $(Ca_{3.00}Y_{0.01})_{\Sigma 3.01}(Sc_{0.63}Ti^{4+}_{0.66}Fe^{3+}_{0.25}Zr_{0.30}Mg_{0.08}Cr^{3+}_{0.06}Fe^{2+}_{0.01})\Sigma_{1.99}(Si_{2.13}Al_{0.26}Fe^{3+}_{0.61})_{\Sigma 3}O_{12}$ composition (Table 1, analysis 15).

The symmetry and cell dimension of the eringaite with the greatest Sc_2O_3 content (holotype specimen, Table 1, analysis 14) was studied using EBSD (Fig. 2). Kikuchi patterns were collected at detector distances (DD) of 150 and 177 mm. The Kikuchi pattern at a DD of 150 mm was fitted to the structural model of synthetic scandian garnet $Ca_3Sc_{1.36}Fe_{0.64}Si_3O_{12}$ with cell parameter a = 12.1917(1) Å (Quartieri *et al*., 2006). Fitting of the EBSD pattern yielded a model with a = 12.19 Å [mean angular deviation (MAD) = 0.22º; excellent fit]. Thus the holotype eringaite specimen is characterized by: a = 12.19 , V = 1811.39 Å^3, Z = 8, $Ia\bar{3}d$. *PowderCell for Windows* version 2.4 (Kraus and Nolze 1996) was used to calculate a powder diffraction pattern of the holotype eringaite (analysis 14, Table 1) for Debye-Scherrer geometry and Co-$K\alpha$ X-radiation (Table 2).

The following Raman bands were found in unpolarized spectra of eringaite (strong bands are underlined, cm^{-1}): 219, 254, 310, 335, 362, 412, 443, 511, 543, 600, 640, 735, 803, 880 and 937

TABLE 2. Calculated XRD pattern of eringaite (for Co-$K\alpha$ and Debye-Scherrer geometry).

h	k	l	D (Å)$_{cal}$	I_{cal}
2	2	0	4.3328	18
4	0	0	3.0637	69
4	2	0	2.7403	100
3	3	2	2.6128	10
4	2	2	2.5015	68
4	3	1	2.4034	14
5	2	1	2.2374	11
6	1	1	1.9880	9
6	2	0	1.9377	12
4	4	4	1.7689	7
6	4	0	1.6995	30
6	4	2	1.6376	82
8	0	0	1.5319	14
8	1	1	1.5085	2
6	5	3	1.4647	1
8	2	2	1.4443	2
8	4	0	1.3701	20
8	4	2	1.3371	19
6	6	4	1.3064	15
8	5	1	1.2918	1
8	4	4	1.2508	2
8	5	3	1.2379	2
10	4	0	1.1378	8
8	6	4	1.1378	13
10	4	2	1.1187	29

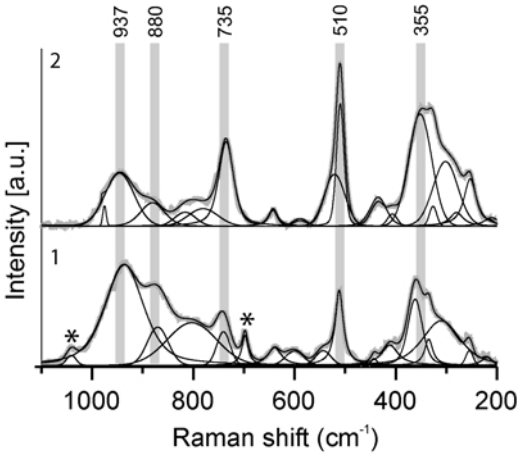

FIG. 3. Raman spectra of eringaite (1) and Sc-Ti-bearing kimzeyite (2). Spectra 1 and 2 were obtained from different zones of the same crystal. Bands induced by impurities of layered magnesian silicates are denoted by asterisks.

(Fig. 3). The positions of the main bands on the Raman spectrum of eringaite are similar to those of kimzeyite and Zr-Sc-bearing schorlomite (Galuskina *et al*., 2005). However, the more intense bands in the range 800–1000 cm^{-1} are characteristic of eringaite, and also of synthetic $Ca_3Sc_2Si_3O_{12}$ (Piccinelli *et al*. 2009).

Discussion

The maximum Sc_2O_3 content (11.20 wt%) found in the Wiluy River eringaite corresponds to 0.82 a.p.f.u. of Sc at the octahedrally coordinated *Y* site according to the formula $Ca_3Y_2Z_3O_{12}$ for calcium garnets. This means that in eringaite the *Y* site is <50% occupied by Sc. However, in this case, the simple 50% rule should not be used for definition of a mineral species as more than three main cations share the octahedral *Y* site. The reader is reminded that the majority of schorlomite species also have Ti < 1 a.p.f.u. at the octahedrally-coordinated *Y* site (Huggins *et al*., 1977; Locock *et al*., 1995; Peterson *et al*., 1995; Chakhmouradian and McCammon, 2005). Considering the recently extended dominant-constituent valence rule (Hatert and Burke, 2008), eringaite and associated garnets can be described in terms of a continuous solid-solution of the three main end-member types: (1) $Ca_3R^{3+}_2Si_3O_{12}$, R^{3+} = Sc, Fe^{3+}, Al, Cr – andradite-like homovalent substitution at the *Y* site; (2) $Ca_3(R^{2+}R^{4+})Si_3O_{12}$, R^{2+} = Mg,Fe^{2+}, R^{4+} = Ti^{4+}(Zr) – morimotoite-like coupled heterovalent substitution at the *Y* site; (3) $Ca_3R^{4+}_2(R^{3+}_2Si)O_{12}$, R^{4+} = Ti^{4+}, Zr, R^{3+} = Fe^{3+}, Al – schorlomite-like coupled heterovalent substitution at the *Y* and *Z* sites (Table 1). In Table 1, the main end-members for each analysed composition are presented based on the dominant cations. Although the crystal used for the single-crystal X-ray data has Ti^{4+} > Sc at the *Y* site, it still has eringaite as the dominant component (Table 1, analysis 15) as the Ti^{4+} content splits into a morimotoite and schorlomite component.

Even if some critics dissent from the extended dominant-constituent rule (Hatert and Burke, 2008), the case for eringaite is unambiguous as the holotype sample characterized by EBSD (Fig. 2) has Sc as the dominant cation at *Y* (Table 1, holotype specimen and analysis 14).

The Raman spectra of eringaite and Sc-Ti-bearing kimzeyite shown in Fig. 3 are similar. The corresponding bands at 937 and 880 cm^{-1} related to symmetric and asymmetric stretching vibrations of SiO_4 tetrahedra appear in the Raman spectra of eringaite and kimzeyite (Kolesov and Geiger, 1998, Schingaro *et al*., 2001). The band at 735 cm^{-1} corresponds to vibrations of $Fe^{3+}O_4$ tetrahedra. Moreover, this band is more intensive in the kimzeyite spectrum than in the eringaite one. In turn, the bands related to vibrations of SiO_4 tetrahedra are more intensive in eringaite spectra. The narrow band at 510 cm^{-1} is attributed to the bending vibrations of SiO_4 tetrahedra. Its position depends upon the ionic radii of the main cations at the octahedrally coordinated *Y* site. This band is placed near 550 cm^{-1} in grossular [$^{VI}Al^{3+}$ 0.535] and near 515 cm^{-1} in andradite [$^{VI}Fe^{3+}$ 0.645] (Kolesov and Geiger, 1998, Schingaro *et al*., 2001). If cations with greater mean ionic radii [^{VI}Zr 0.72, ^{VI}Mg 0.72, ^{VI}Sc 0.745, $^{VI}Fe^{2+}$ 0.78 Å] prevail at *Y*, this band will shift further towards lower frequencies. In the case of the Sc-rich garnets from the Wiluy River area, it is placed near 510 cm^{-1} even when measured in different zones of the same crystal. For example, the band related to $R(ZO_4)^{4-}$ vibrations near 355 cm^{-1} is near 310 cm^{-1} in kimzeyite (Schingaro *et al*., 2001), near 373 cm^{-1} in grossular-andradite and near 376 cm^{-1} in $Ca_3Sc_2Si_3O_{12}$ (Piccinelli *et al*., 2009). In our case, when a small amount of the Si [0.26 Å] at *Z* is substituted by the larger cations Al [0.39 Å] and Fe^{3+} [0.44 Å], that band shifts

towards lower frequencies relative to the corresponding band in silicate garnets.

The unique crystallization of eringaite in the Wiluy River area is associated with a high-temperature process of skarn formation. At this locality, a large xenolith (>200 m) of Ordovician sedimentary carbonate rocks in the Triassic gabbro-dolerite intrusion of the Siberian trap formation was metamorphosed under sanidinite-facies conditions at temperatures >800ºC (Galuskin, 2005; Galuskina *et al*., 2005). As with the formation of exotic zirconian and stannian garnets such as bitikleite-(SnAl), bitikleite-(ZrFe), toturite and elbrusite-(Zr) in near-surface, high-temperature skarns in the Caucasus (Galuskina *et al*., 2010*a*–*c*), the $^{IV}Fe^{3+}$-dominant analogue of kimzeyite represents the earliest garnet of the Wiluy River skarns. It possibly enabled incorporation of relatively large cations such as Sc, Sn^{4+} and U^{6+} at the octahedrally-coordinated *Y* site of later garnet growing epitactically or metasomatically as zones on the primary Zr garnet. I.G. and E.G. acknowledge financial support by the Ministry of Science and Higher Education of Poland, grant Nr N307 097038.

References

Chakhmouradian, A.R. and McCammon, C.A. (2005) Schorlomite: a discussion of the crystal chemistry, formula, and inter-species boundaries. *Physics and Chemistry of Minerals*, **32**, 277–289.

Chen, Y., Gong, M. and Cheah, K.W. (2009) Effects of fluxes on the synthesis of $Ca_3Sc_2Si_3O_{12}$:Ce^{3+} green phosphors for white light-emitting diodes. *Materials Science and Engineering*, **B**, doi:10.1016/j.mseb.2009.09.024.

Cooper, M.A., Hawthorne, F.C., Ball, N.A., Černý, P. and Kristiansen, R. (2006) Oftedalite, $(Sc,Ca,Mn^{2+})_2K(Be,Al)_3Si_{12}O_{30}$, a new member of the milarite group from the Heftetjern pegmatite, Tordal, Norway: Description and crystal structure. *The Canadian Mineralogist*, **44**, 943–949.

Day, A. and Trimby, P. (2004) *Channel 5 Manual HKL Technology Inc*., Hobro, Denmark.

Demartin, F., Gramaccioli, C.M. and Pilati, T. (2000) Structure refinement of bazzite from pegmatitic and miarolitic occurrences. *The Canadian Mineralogist*, **38**, 1419–1424.

Galuskin, E.V. (2005) *Minerals of the vesuvianite group from achtarandite rocks (Wiluy River, Yakutia). Series of wiluite-vesuvianite-Si-deficient vesuvianite hydrovesuvianite. Genesis of achtarandite rodingitoids* (in Polish), University of Silesia, Katowice, Poland.

Galuskina, I.O., Galuskin, E.V. and Sitarz, M. (1998) Atoll hydrogarnets mechanism of the formation of achtarandite pseudomorphs. *Neues Jahrbuch für Mineralogie Monatshefte*, 1998(**2**), 49–66.

Galuskina, I.O., Galuskin, E.V., Dzierżanowski, P., Armbruster, T. and Kozanecki, M. (2005) A natural scandian garnet. *American Mineralogist*, **90**, 1688–1692.

Galuskina, I.O., Galuskin, E.V., Armbruster, T., Lazic, B., Dzierżanowski, P., Gazeev, V.M., Prusik, K., Pertsev, N.N., Winiarski, A., Zadov, A.E., Wrzalik, R. and Gurbanov, A.G. (2010*a*) Bitikleite-(SnAl) and bitikleite-(ZrFe) – new garnets from xenoliths of the Upper Chegem volcanic structure, Kabardino-Balkaria, Northern Caucasus, Russia. *American Mineralogist* (in press).

Galuskina, I.O., Galuskin, E.V., Armbruster, T., Lazic, B., Kusz, J., Dzierżanowski, P., Gazeev, V.M., Pertsev, N.N., Prusik, K., Zadov, A.E., Winiarski, A., Wrzalik, R. and Gurbanov, A.G. (2010*b*) Elbrusite-(Zr) – a new uranian garnet from the Upper Chegem caldera, Kabardino-Balkaria, Northern Caucasus, Russia. *American Mineralogist* (in press).

Galuskina, I.O., Galuskin, E.V., Dzierżanowski, P., Gazeev, V.M., Prusik, K., Pertsev, N.N., Winiarski, A., Zadov, A.E. and Wrzalik, R. (2010*c*) Toturite $Ca_3Sn_2Fe_2SiO_{12}$ – a new mineral species of the garnet group. *American Mineralogist* (in press).

Gramaccioli, C.M., Campostrini, I. and Orlandi, P. (2004) Scandium minerals in the miaroles of granite at Baveno, Italy. *European Journal of Mineralogy*, **16**, 951–956.

Groat, L.A., Hawthorne, F.C., Ercit, T.S. and Grice, J.D. (1998) Wiluite $Ca_{19}(Al,Mg,Fe,Ti)_{13}(B,Al,)_5Si_{18}O_{68}(O,OH)_{10}$, a new mineral species isostructural with vesuvianite, from the Sakha Republic, Russian Federation. *The Canadian Mineralogist*, **36**, 1301–1304.

Hatert, F. and Burke, E. (2008) The IMA-CNMNC dominant-constituent rule revised and extended. *The Canadian Mineralogist*, **46**, 717–728.

Huggins, F.E., Virgo, D. and Huckenholz, H.G. (1977) Titanium-containing silicate garnets. II. The crystal chemistry of melanites and schorlomite. *American Mineralogist*, **62**, 646–665.

Ito, J. and Frondel, C. (1968) Synthesis of the scandium analogues of aegirine, spodumene, andradite and melanotekite. *American Minerologist*, **53**, 1276–1280.

Ivanovskikh, K.V., Meijerink, A., Piccinelli, F., Speghini, A., Zinin, E.I., Ronda, C. and Bettinelli, M. (2010) Optical spectroscopy of $Ca_3Sc_2Si_3O_{12}$, $Ca_3Y_2Si_3O_{12}$ and $Ca_3Lu_2Si_3O_{12}$ doped with Pr^{3+}. *Journal of Luminescence*, **130(5)**, 893–901.

Kolesov, B.A. and Geiger, C.A. (1998) Raman spectra

of silicate garnets. *Physics and Chemistry of Minerals*, **25**, 142–151.

Kraus, W. and Nolze, G. (1996) POWDER CELL – a program for the representation and manipulation of crystal structures and calculation of resulting X-ray powder patterns. *Journal of Applied Crystallography*, **29**, 301–303.

Lyakhovich, V.V. (1954) New mineralogical data from the Wiluy achtarandite deposit. *Trudy Vostochno-Sibirskogo filiala Akademii Nauk SSSR, Seria Geologicheskaya*, **1**, 85–116 (in Russian).

Locock, A.J. (2008) An Exel spreadsheet to recast analyses of garnet into end-member components, and a synopsis of the crystal chemistry of natural silicate garnets. *Computers Geoscience*, **34**, 1769–1780.

Locock, A., Luth, R.W., Cavell, R.G., Smith, D.G.W. and Duke, M.J.M. (1995) Spectroscopy of the cation distribution in the schorlomite species of garnet. *American Mineralogist*, **80**, 27–38.

Ma, C. and Rossman, G.R. (2009) Davisite, $CaScAlSiO_6$, a new pyroxene from the Allende meteorite. *American Mineralogist*, **94**, 845–848.

Mellini, M., Merlino, S., Orlandi, P. and Rinaldi, R. (1982) Cascandite and jervisite, two new scandium silicates from Baveno, Italy. *American Mineralogist*, **67**, 599–603.

Mill', B.V. (1964) Hydrothermal synthesis of garnets containing V^{3+}, In^{3+}, and Sc^{3+}. *Doklady Akademii Nauk SSSR*, **156(4)**, 814–816 (in Russian).

Mill', B.V. (1966) Hydrothermal synthesis of silicates and germanates with garnet-type structure. *Zhurnal Neorganicheskoi Khimii, XI*, **7**, 1533–1538 (in Russian).

Mill', B.V., Belokoneva, E.L., Simonov, M.A. and Belov, N.V. (1977) Refined crystal structures of the scandium garnets $Ca_3Sc_2Si_3O_{12}$, $Ca_3Sc_2Ge_3O_{12}$ and $Cd_3Sc_2Ge_3O_{12}$. *Zhurnal Strukturnoi Khimii*, **18**, 399–402 (in Russian).

Offman, P.F. and Novikova, A.S. (1955) Volcanic pipe Eringa. *Izvestiya Akademii Nauk SSSR, Seria Geologicheskaya*, **4**, 121–139 (in Russian).

Oleynikov, B.V. (1979) *Geochemistry and Ore Genesis of Platform Basites*. Nauka, Novosibirsk (in Russian).

Orlandi, P., Pasero, M. and Vezzalini, G. (1998) Scandiobabingtonite, a new mineral from the Baveno pegmatite, Piedmont, Italy. *American Mineralogist*, **83**, 1330–1334.

Peterson, R.C., Locock, A.J.A. and Luth, R.W. (1995) Positional disorder of oxygen in garnet: The crystal-structure refinement of schorlomite. *The Canadian Mineralogist*, **33**, 627–631.

Pezzotta, F., Diella, V. and Guastoni, A. (2005) Scandium silicates from the Baveno and Cuasso al Monte NYF-granites, southern Alps (Italy): Mineralogy and genetic inferences. *American Mineralogist*, **90**, 1442–1452.

Piccinelli, F., Speghini, A., Mariotto, G. and Bettinelli M. (2009) Visible luminescence of lanthanide ions in $Ca_3Sc_2Si_3O_{12}$ and $Ca_3Y_2Si_3O_{12}$. *Journal of Rare Earths*, **72**, 4, 555–559.

Pouchou, J.L. and Pichoir, F. (1985) "PAP" (Z) procedure for improved quantitative microanalysis. Pp. 104–106 in: *Microbeam Analysis – 1985*. San Francisco Press, San Francisco, California, USA.

Prendel, R. (1887) About wiluite. *Proceeding of Novorossiysk society of nature investigator*, **XII**, **2**, 1–48 (in Russian).

Quartieri, S., Oberti, R., Boiocchi, M., Dalconi, M.C., Boscherini, F., Safonova, O. and Woodland A.B. (2006) Site preference and local geometry of Sc in garnets: Part II. The crystal-chemistry of octahedral Sc in the andradite-$Ca_3Sc_2Si_3O_{12}$ join. *American Mineralogist*, **91**, 1240–1248.

Raade, G., Ferraris, G., Gula, A., Ivaldi, G. and Bernhard, F. (2002) Kristiansenite, a new calcium-scandium-tin sorosilicate from granite pegmatite in Tordal, Telemark, Norway. *Mineralogy and Petrology*, **75**, 89–99.

Semenov, I.E., Khomyakov, A.R. and Bukova, A.V. (1965) Magbasite – new mineral. *Doklady Akademii Nauk SSSR*, **163**(3), 718–719 (in Russian).

Schingaro, E., Scordari, F., Capitano, F., Parodi, G., Smith, D.C. and Motana, A. (2001) Crystal chemistry of kimzeyite from Anguillara, Mts. Sabatini, Italy. *European Journal of Mineralogy*, **13**, 749–759.

Werner G.A. (1811) *Handbuch der Mineralogie*. Hofmann, **1**, pp. 479.

Woodland, A.B. and Angel, R.J. (1996) Synthesis and properties of $Ca_3Fe_2Si_3O_{12}$–$Ca_3Sc_2Si_3O_{12}$ garnet solid solutions. *Terra Abstracts*, **8**, 68.